

CELL ADHESION STATUS-DEPENDENT HISTONE ACETYLATION IS REGULATED THROUGH INTRACELLULAR CONTRACTILITY-RELATED SIGNALING ACTIVITIES

Yong-Bae Kim¹, Jiyon Yu¹, Sung-Yul Lee², Mi-Sook Lee², Seong-Gyu Ko¹, Sang-Kyu Ye³ Hyun-Soon Jong¹, Tae-You Kim^{1,2}, Yung-Jue Bang^{1,2}, and Jung Weon Lee^{1,2} Cancer Research Institute, Departments of ¹Tumor Biology, ²Molecular and Clinical Oncology, and ³Pharmacology, College of Medicine, Seoul National University, Seoul 110-799, Korea.

Running title: cell adhesion status-dependent histone acetylation.

Address correspondence to: Jung Weon Lee, Cancer Research Institute, Departments of Tumor Biology, and Molecular & Clinical Oncology, College of Medicine, Seoul National University, 28, Yeongeong-dong, Jongno-gu, Seoul 110-799, Korea, Tel. 82-2-3668-7030; Fax. 82-2-766-4487; E-mail: jwl@snu.ac.kr

Although histone acetylation is important for epigenetic gene transcription, their regulation by extracellular cues has rarely been evidenced. Here, we examined whether and how histone acetylation is regulated by cell adhesion-mediated signaling. Gastric carcinoma cells in suspension showed a higher histone acetylation, compared to fibronectin-adherent cells. This difference was supported by a decreased histone deacetylases (HDACs) activity. Furthermore, trichostatin A (TSA)-mediated histone acetylation was significantly increased only in suspended, but not in fibronectin-adherent, cells. Pharmacological inhibition of intracellular contractility-related myosin light chain kinase (MLCK) or RhoA-kinase (ROCK) or expression of ROCK1 siRNA, dominant negative RhoA or active Rac1 decreased basal and TSA-mediated histone H3 acetylations in suspended cells, whereas inhibition of calmodulin-dependent protein kinase II (CaMKII) or transient overexpression of wild type MLCK enhanced the acetylations. Meanwhile, chromatin immunoprecipitation showed higher basal and TSA-enhanced associations of ROCK1 promoter regions with (Lys9-) acetylated histone 3 in suspended cells than in fibronectin-adherent cells and expression of ROCK1 was higher and further increased by TSA treatment in suspension. In addition, phosphorylation of myosin light chain was further increased by TSA in suspension and higher in anchorage-independent cells over adherently-growing cells, indicating an inverse relationship between ROCK1

expression (-mediated contractility) and cell adhesion abilities. Cell adhesion analysis showed that pharmacological activation of intracellular contractility-related signaling activities decreased cell adhesion abilities, whereas inhibition of them increased the adhesion. Taken together, these observations suggest that cell adhesion-related signal transduction regulates histone acetylation, presumably through a close functional linkage between intracellular contractility and HDACs activity/histone acetylation.

Adhesion and spreading through integrin-mediated engagements to extracellular matrix (ECM) enable cells to trigger diverse intracellular signal transduction, leading to regulation of diverse cellular behaviors (1-4) including gene expression (5,6).

Gene transcription is a highly coordinated and orchestrated cellular process, which ensures that genes are induced or suppressed as their respective proteins are needed for their cellular functions. In contrast to genetic mechanisms involving changes in DNA sequences, epigenetic transcriptional regulation mechanisms define all heritable changes in gene expression that are not coded in the DNA sequence itself. As an epigenetic process, histone acetylation has recently been extensively studied (7-10). The N-terminals of histone H3 or H4 tails wrapping a nucleosome were shown to be targeted by various molecules with histone acetyltransferase (HAT) or deacetylase (HDAC) activity. The histone acetylation may alter the compactness of a nucleosome relative to neighboring nucleosomes, leading to the allowance or

prohibition of approaches of transcriptional machineries consisting of transcription factors and cofactors (11,12). Among the amino acid residues of H3, acetylation of Lys9 is well-known to be transcription permissive (13).

Intracellular contractility depends on phosphorylation degree of a 20 kD myosin light chain (MLC), for which signal transduction pathways have been identified (14,15). MLCK is a kinase that phosphorylates MLC in cortical actin bundles, and the binding of this phosphorylated MLC to actin forms actomyosin complexes and leads to their contraction (14). MLCK is activated by Ca^{++} /Calmodulin, but also becomes inactive through its phosphorylation by calmodulin-dependent protein kinase II (CaMKII) (14). ROCK also phosphorylates the MLC in stress fibers and inactivates MLC phosphatases, resulting in cellular contractility (16). ROCK is activated through cell adhesion signal transduction involving RhoA GTPase and importantly function in regulation of intracellular contractility (17).

One previous study reported that CaMK phosphorylated HDAC5, leading to its nuclear export and thus MEF2-dependent transcription of genes for muscle differentiation (18). Although active investigations on the epigenetic gene transcription have recently been conducted, the effects of the extracellular cues on regulation of epigenetic processes have received very little attention.(19). Cell adhesion regulates gene transcription in the nucleus (5). We hypothesized that intracellular signaling activity depending on integrin-mediated cell adhesion status may regulate enzyme quantity and activity of HATs and HDACs, which in turn modulate histone acetylations and thereby gene transcription. To test this possibility, we analyzed the levels and activities of HDACs, acetylations of histones in suspended and adherent conditions, the activities of intracellular contractility-related signaling molecules, and their biological significance, using gastric carcinoma cells. The observations made revealed that cell adhesion-related signal transduction can indeed modulate histone acetylation, presumably through a close functional connection between intracellular contractility and HDACs activity/histone acetylation.

EXPERIMENTAL PROCEDURES

Cells: Gastric carcinoma SNU16mAd (20) cells were maintained in RPMI-1640 containing 10% fetal bovine serum in a humidified CO₂ incubator (5% CO₂ and 37°C).

Transient transfection: SUN16mAd cells were transiently transfected with either mock control vector, pcDNA3-MLCK WT, pZip Rac1 Q61L (an active form), or pZip RhoA T19N (a dominant-negative form), control GFP siRNA (QIAGEN, Catalog No of 1022079), or ROCK1 siRNA (Dharmacon, Lafayette, CO, USA, catalogue number of M-003536-01-0005, human ROCK1 of NM-005406) using Lipofectamine 2000TM (Invitrogen) according to manufacture's protocols. Cells were kept in suspension or replated on fibronectin-precoated dishes, 24 h after the transfections.

Replating cells on fibronectin: Cell manipulation to keep in suspension or replating in the absence of serum was done as explained previously (21). Except for the indicated replating periods, cells were kept in suspension or replated on fibronectin- (10 µg/ml, Chemicon) precoated culture dishes for 20 h. Cell aggregation by keeping cells in suspension for 20 h was not allowed presumably by virtues of 1% BSA in the replating media and rolling (80 rpm) during the incubation. Pharmacological inhibitors such as TSA, cytochalasin D, Y27632, ML9, KN93, MLCK inhibitory peptide p18 (Tocris Cookson Ltd., Avonmouth, UK), lysophosphatidic acid (LPA), okadaic acid (Sigma), KN92, and Calmidazolium-Cl (Merck) were pretreated 30 min before the cell replating. Cells were collected for extract preparation after incubation for 20 h or the indicated periods at 37°C in 5% CO₂.

Preparation of whole cell extracts or nuclear extracts: Whole cell extracts were prepared as described previously (22). Nuclear extracts were prepared, based on previously described methods (23). Briefly, suspended cells were spun down and adherent cells were trypsinized quickly before collection. The cells were twice washed with ice-cold PBS, and then the cell pellets were resuspended with Nuclei Isolation Buffer (NIB, 15 mM Tris-HCl, pH 7.5, 60 mM KCl, 15 mM NaCl, 5 mM MgCl₂, 1 mM CaCl₂,

1 mM DTT, 2 mM Na₃VO₄, 250 mM sucrose, 1 mM leupeptin, 1 mM aprotinin, 1 mM pepstatin A, and 2 mM PMSF, 500 µl/10 cm dish). Next another 500 µl of NIB containing 0.6% NP-40 was added and the mixture was incubated on ice for 5 min before spinning at 2000 x g for 5 min at 4°C. Then the supernatant was decanted and the pellets were washed with NIB again. The pellets were then resuspended with a little amount (< 200 µl/10 cm dish) of Nuclei Extract Buffer (NEB, 25 mM Tris-HCl, pH 8.0, 250 mM NaCl, 1 mM EDTA, 10% glycerol, 0.2% NP-40, 1 mM leupeptin, 1 mM aprotinin, 1 mM pepstatin A, and 2 mM PMSF). Then DNase (250 units/condition) and 5 mM MgCl₂ were added prior to an incubation on ice for 1 h. After the incubation, 10 mM EDTA (final concentration) was added and the mixtures were spun at 13000 rpm for 30 min at 4°C. The supernatant were taken for nuclear extracts.

Western Blots: Standard western blottings and stripping of membranes were done as explained previously (21). The primary antibodies used included anti-acetylated H3, Lys9-acetylated H3, HDACs 1 to 6 (Upstate Cell Signaling, Lake Placid, NY), MLCK (Sigma), RhoA, Rac1 (BD transduction Lab., San Jose, CA), α-tubulin, H3, phospho-MLC, and ROCK1 (Santa Cruz Biotech. Inc., Santa Cruz, CA).

HDAC activity assay: HDAC activity assays were performed using a HDAC fluorescent activity assay kit, as instructed by the manufacture (Biomol[®], AK-500 kit). The deacetylation of the *Fluor de Lys* substrate in the kit by active HDACs in samples sensitizes to the developer in the kit, which then generates a fluorophore. A positive control (a HeLa extract supplied in the kit) and a negative control (a mixture of HeLa extract and TSA) were included by a parallel manner. The fluorophore was excited at 360 nm and emitted fluorescence (460 nm) was detected using a LS55 spectrometer (Perkin Elmer).

RT-PCR: Total RNAs from cells under the indicated conditions were extracted with the Trizol reagent (Gibco BRL), following manufacture's protocols. cDNAs were synthesized from 1 µg of total RNA using MMLV reverse transcriptase (Invitrogen) with 250 ng random hexamers. ROCK1 cDNA was amplified by PCR using a sense (5'-ATG ATG

TGC CTG AAA AAT GGG-3') primer and an antisense (5'-AAA AAT ACC CCA ACC GAC CAC-3') primer. Reactions were performed in 20 µl under the following conditions: 94°C for 5 min; then 35 cycles of 94°C for 30 sec, 54°C for 30 sec, and 72°C for 30 sec; and finally 10 min at 72°C. GAPDH was used as an internal control. Standard agarose gel electrophoresis was performed to visualize the PCR products.

Chromatin immunoprecipitation (ChIP): ChIP was performed as explained previously (24). Briefly, SNU16mAd cells were fixed with formaldehyde for 15 min at room temperature. Soluble chromatin was immunoprecipitated with 2 µg of anti-acetylated H3 or Lys9-acetylated H3 (Upstate Biotechnology, Lake Placid, NY) overnight. The same set of input DNA and 5% of purified ChIP DNA were subjected to quantitative PCR with ROCK1 primers for 30 cycles. A sense (5'-ATT CTT CCC AGT CAA GCC TG-3') and an antisense (5'-TAT CAG CTC TAG GCA AAA GC-3') ROCK1 primer were used. Standard agarose gel electrophoresis was performed to visualize the PCR products.

Cell adhesion assay: The cell adhesion on fibronectin was examined as previously described (25). Before being replated on fibronectin-precoated 96 well plates, cells were pretreated with KN93 (20 µM), LPA (10 µM), Cytochalasin D (1 µM), ML9 (25 µM), Y27632 (15 µM), or MLCK inhibitory peptide p18 (5 µM). Cells replated were incubated at 37°C, 5% CO₂ for 15 h, before washings, fixation, and staining adherent cells with crystal violet as explained previously (25). After staining of adherent cells and washings, the degree of staining was eventually read at 564 nm by a microplate reader, to indicate the relative cell adhesion (adhesion in each condition subtracted with adhesion on BSA-precoated wells). Five wells were handled in parallel and the middle three values were averaged for each condition. Data shown (mean ± standard deviation) were representative from three different assays.

Statistical analysis: Band intensities were quantitated by a densitometer from 3 independent experiments and the mean and standard deviation (SD) values were calculated for student *t*-tests after normalization to H3 or α-

tubulin intensities. The mean values of band intensities were shown under the representative blots. Paired student's *t*-tests were performed for comparisons of mean values to see if the difference is significant. *p* values ≤ 0.05 were considered significant.

RESULTS

Cell adhesion status-dependent HDACs activity and histone acetylation

To examine the role of cell adhesion in epigenetic gene transcription, we first examined acetylation levels of H3 in suspended or fibronectin-adherent cells. During preliminary experiments, we found that gastric carcinoma SNU16mAd cells required replating on fibronectin for longer than 6 ~ 8 h to be adherent enough for nuclear extraction and biochemical analysis (data not shown). Cells were maintained either in suspension or replated on fibronectin-coated culture dishes in serum-free media, and incubated them for 8, 12, or 20 hr at 37°C in 5% CO₂. Cells in suspension showed markedly higher acetylation levels in H3 and H3 Lys9 (K9-H3), compared to fibronectin-adherent cells, although the total H3 levels in the extracts were similar under suspended or adherent conditions (Figure 1A). Next we examined if the differential H3 and K9-H3 acetylations correlated with different expression levels of HDACs. Nuclear extracts from suspended or fibronectin-adherent cells were analyzed for class I HDACs (mostly nuclear HDAC1, 2, and 3) and class II shuttling between nucleus and cytosol (HDAC 4, 5, and 6) (26). However, the levels of certain HDACs responsible for histone deacetylation were similar (Figure 1B). Next, we tested whether enzymatic activities of HDACs were responsible for the higher histone acetylation in suspended cells, compared to fibronectin-adherent cells. Adherent cells showed higher HDACs activity, compared to suspended cells (Figure 1C), and positive and negative controls showed the expected activities (Figure 1C). This higher activity in adherent cells correlated with the lower acetylation levels of H3 and K9-H3 in adherent cells. Therefore, it is likely that, depending on cell adhesion status, SNU16mAd cells may adopt different mechanism(s) to regulate HDAC activity and

thus histone acetylation.

TSA-sensitive histone acetylation occurred only in suspended cells

It is well-known that TSA is a potent inhibitor of HDACs (27). Therefore, we examined how cell adhesion status-dependent H3 and K9-H3 acetylations might respond to TSA treatment. Interestingly, TSA treatment of suspended cells further increased acetylations in H3, whereas TSA treatment of fibronectin-adherent cells caused no significant changes in H3 acetylation (Figure 2A). Acetylation of H3 Lys9 (Ac-K9-H3) was also increased by TSA treatment only in suspended cells, although the total H3 level was very similar in the nuclear extracts (Figure 2A). Other HDACs inhibitors such as SAHA and sodium butyrate also regulated the acetylations, as TSA did (data not shown). Expression levels of HDACs 1 to 6 were similar in suspended and adherent cells. This differential acetylation of H3 and K9-H3 dependence on cell adhesion status was also apparent at earlier time points, such as 8 h either in suspension or adherent (data not shown). This TSA-mediated increase in H3 and K9-H3 acetylation correlated with a significant TSA efficiency to down-regulate HDACs activity in suspended cells (Figure 2B). In contrast, no change in TSA-mediated acetylation in adherent cells was supported by an insignificant TSA treatment efficiency (Figure 2B). The lack of change in TSA-mediated acetylation in fibronectin-adherent cells might be because adhesion signaling was not sufficient for SNU16mAd cells to show the TSA response. Such an explanation may be possible, because different signaling contexts caused an increase in H3 and K9-H3 acetylations even in adherent cells. Treatment with cytochalasin D (an actin depolymerizing agent) or okadaic acid (an inhibitor of Ser/Thr phosphatases) resulted in H3 acetylation even in adherent cells (Figure 2C). However, HDAC1, 2, and 3 levels, but not total H3, were unequal depending on okadaic acid treatment, presumably indicating intracellular trafficking (28) or degradation. These findings suggest that in the carcinoma cells we tested histone acetylation is TSA-sensitive in suspended cells, and TSA-insensitive in fibronectin-adherent cells.

Intracellular contractility-related signaling

activity regulates the histone acetylation

Intracellular signaling activities involved in the cell adhesion status-dependent regulation of histone acetylation were examined. Pharmacological inhibitors were tested using suspended and adherent cells. Among the inhibitors, we observed significantly decreased acetylations in suspended cells and increased acetylations in fibronectin-adherent cells by ML9 (a specific MLCK inhibitor) (Figure 3A). In both cell conditions, the total H3 levels in each extract were very similar (Figure 3A). These ML9-induced decreases in basal and TSA-sensitive acetylations in suspended cells appeared to be due to HDACs activities increased by ML9 treatment (2 ~ 4 folds increased, Figure 3B). The slight increases observed in ML9-induced acetylations in fibronectin-adherent cells, compared to ML9-treated suspended cells, correlated with a ML9-induced decrease in HDACs activity (about 20% reduced, Figure 3C).

We next examined the effects of MLCK overexpression on the histone acetylations. Cells were transiently transfected with a control or MLCK cDNA plasmid, 24 h prior to cell replating. Exogenous expression of MLCK caused an increase in phosphorylation of myosin light chain (p-MLC), indicating an increase in intracellular contractility (Figure 3D). Furthermore, MLCK overexpression increased basal and TSA-induced H3 and K9-H3 acetylations in suspended cells, whereas in adherent cells barely detectable acetylations were at best diminished or not changed by MLCK overexpression, although the total H3 levels in the extracts were similar (Figure 3D).

Since MLCK is known to be negatively regulated by CaMKII (14), we investigated if CaMKII inhibition might affect the histone acetylations in suspended or fibronectin-adherent cells. Basal and TSA-induced H3 and K9-H3 acetylations in suspended cells were further enhanced by KN93 (a specific CaMKII inhibitor) treatment, whereas no significant change at a hardly detectable level was seen in fibronectin-adherent cells (Figure 3E). However, the total H3 levels were similar in the nuclear extracts from either suspended or adherent cells (Figure 3E). Meanwhile, KN92 (a negative control compound of KN93) did not

cause any significant changes in the acetylations (Figure 3F). On the other hand, a calmodulin (CaM) antagonist, calmidazolium, caused alteration in the acetylations; suspended cells treated with calmidazolium reduced the acetylations, whereas fibronectin-adherent cells with calmidazolium treatment caused increased acetylations (Figure 3G), indicating the significance of CaM in regulation of contractility-related signaling activity and thereby cell adhesion status-dependent-acetylations.

RhoA GTPase is also known to regulate intracellular contractility through regulation of actin polymerization (17). Exogenous expression of dominant negative RhoA (leading to inhibition of contractility, see Figure 7) reduced the acetylations in suspended cells, whereas it did not cause any changes at a barely detectable level in fibronectin-adherent cells, although the total H3 detected similarly in the extracts (Figure 4A). In addition, inhibition of ROCK1 (a downstream effector of RhoA) by Y27632 also reduced basal and TSA-sensitive acetylations in suspended cells, whereas it caused slight increases in the acetylations in fibronectin-adherent cells, although the total H3 levels were similar in the nuclear extracts from both suspended and adherent cells (Figure 4B). Furthermore, suppression of ROCK1 by using its siRNA pool resulted in reduced acetylations in suspended cells but increases in the adherent cells (Figure 4C). In contrast to RhoA GTPase, Rac1 GTPase is often shown to relieve actin stress tension, via an action antagonistic against RhoA (29,30). Therefore, we next tested the effect of active Rac1 (Q61L) on H3 and K9-H3 acetylations. Transient transfection of Rac1 Q61L resulted in reductions in the basal and TSA-mediated H3 and K9-H3 acetylations in suspended cells, whereas it slightly increased (Figure 4D). However, the acetylations in fibronectin-adherent cells increased by Rac1 Q61L expression were not sensitive to TSA, just like the fibronectin-adherent cells with the other approaches to regulate contractility-related signaling activities (Figures 3 and 4). In addition to the TSA-insensitive acetylations in the adherent cells without or with approaches to regulate the signaling activity, the acetylations even in suspended cells showed a tendency to

lose the TSA-sensitivity by treatment ML9, calmidazolium or Y27632, or activation of Rac1, although other approaches still maintained the TSA-sensitivity at up- or down-regulated acetylation levels in suspended cells. Therefore, complicated signaling activities regulating intracellular contractility appear to be involved in regulation of H3 and K9-H3 acetylations, differentially depending on cell adhesion status.

Correlation of the histone acetylation with cell adhesion status-dependent ROCK1 expression

We next examined whether histone acetylation might correlate with expression of contractility-related molecules. Oligonucleotide microarray experiments were performed three times and found transcription for ROCK1 decreased on adhesion (data not shown). Thus, chromatin immunoprecipitation approaches were performed to exam association of ROCK1 promoter regions with (Lys9-) acetylated H3. Being consistent with the cell adhesion status-dependent histone acetylation pattern, chromatin immunoprecipitation using anti-acetylated H3 or Lys9-acetylated H3 antibodies resulted in more co-precipitation of ROCK1 promoter regions that further enhanced by TSA treatment in suspended cells, compared to in fibronectin-adherent cells (Figure 5A). Furthermore, mRNA for ROCK1 was higher and further enhanced by TSA treatment in suspension, whereas it was not significantly changed at a minimal level in fibronectin-adherent conditions (Figure 5B), being consistent with the cell adhesion status-dependent histone acetylation pattern. However, a parallel RT-PCR for GAPDH as a control showed a similar level of GAPDH mRNA independent of cell adhesion status (Figure 5B). ROCK1 protein levels were also consistent with the mRNA levels (Figure 5C). Its TSA-mediated increase in suspended cells furthermore correlated with an increased phosphorylation of MLC (Figure 5D), indicating an increased intracellular contractility. Therefore, histone acetylation under control by intracellular contractility appeared to regulate back the contractility through transcription of signaling molecules including ROCK1, indicating a close linkage between histone

acetylation and intracellular contractility (and/or -related signaling activity) in the SNU16mAd cells.

An inverse relationship of intracellular contractility with cell adhesion ability

The increased transcription of ROCK1 by TSA treatment depended on cell adhesion status, indicating a role for ROCK1 in cell adhesion. We thus tested if ROCK1 was differentially expressed between mostly anchorage-independent parental SNU16 cells and adherently-growing SNU16mAd variant cells under normal culture conditions. ROCK1 was expressed higher in SNU16 than SNU16mAd cells, leading to a higher MLC phosphorylation and probably thus contractility (Figure 6A). This indicates an inverse relationship between ROCK1 level (-mediated contractility) and cell adhesion ability. Next we examined if intracellular contractility-related signaling activities correlate inversely with cell adhesion. Adhesion abilities were analyzed using conditions where intracellular contractility might be up- or down-regulated by pharmacological inhibitors. SNU16mAd cells were pretreated without or with diverse inhibitors prior to being replated on fibronectin. The incubation on fibronectin lasted for 15 h, shorter than the usual 20 h, since we might not observe increased cell adhesion in a certain drug-treated condition just due to almost saturated adhesion by the 20 h incubation on fibronectin alone. Activation of intracellular contractility by CAMKII inhibition (KN93), RhoA activation (LPA), or disruption of actin organization (cytochalasin D) decreased the ability of cell adhesion onto fibronectin, whereas contractility inhibition through inhibition of ROCK1 (Y27632) or MLCK (ML9 or p18) increased the adhesion (Figure 6B). These support the idea that the contractility inversely correlates with abilities for cell adhesion onto fibronectin.

Taken together, these observations suggest that cell adhesion status-dependent intracellular contractility signaling may closely link to regulation of HDACs activity and thus histone acetylation in cells we tested.

DISCUSSION

Although extensive studies on epigenetic

gene regulation have recently been undertaken for cancer therapy purposes, its regulation by extracellular signal transduction has rarely been reported. In this study, we explored the effects of cell adhesion and downstream signal transduction on histone acetylation, a key process of epigenetic gene expression regulation.

We observed that SNU16mAd gastric carcinoma cells in suspension showed higher basal and TSA-sensitive H3 and K9-H3 acetylations presumably due to lower HDACs activity, compared to fibronectin-adherent cells. These observations were valid also in cases that AGS and HT29 carcinoma cells were replated on fibronectin for 20 h (data not shown). The cell adhesion status-dependent histone H3 and K9-H3 acetylations were regulated by intracellular contractility-related signaling activities. The histone H3 and K9-H3 acetylations correlated with ROCK1 expression in a cell adhesion-status dependent manner, leading to a higher contractility in suspension. Furthermore, activation of contractility-related signaling decreased the cell adhesion abilities, whereas inhibition significantly increased them. Therefore, observations from this study suggest that cell adhesion status-dependent intracellular contractility signaling activities regulate HDACs activity, histone H3 and K9-H3 acetylations, and expression of genes related to contractility maintenance in the cells we tested. Specifically, chromatin immunoprecipitation of ROCK1 promoter regions demonstrated that the TSA-insensitive deacetylation of (Lys9-) H3 in the fibronectin-adherent cells showed functional consequences leading to regulation of the ROCK1 gene promoter. Therefore, epigenetic regulation of ROCK1 expression appears to be a mechanism to promote cell adhesion, since ROCK1 inhibited cell adhesion.

This current study supports the role of intracellular contractility-related signaling activities in the cell adhesion status-dependent regulation of the histone acetylations. Previously CaMK was shown to phosphorylate HDAC5 and cause nuclear exports leading to MEF2-mediated-transcription for muscle differentiation (18). CaMK is involved in the regulation of intracellular contractility (14). Therefore, the regulation of HDAC activity and/or function appears to occur via alteration of

intracellular contractility (-related signaling activities), as shown in this study. Furthermore, this study presents evidence that the contractility-mediated regulation of HDAC activity and histone acetylation depends on cell adhesion status. It was shown that down-regulation of intracellular contractility, through MLCK inhibition by ML9, CaM inhibition by calmidazolium, ROCK1 inhibition by Y27632, ROCK1 suppression by its siRNA, exogenous expression of dominant negative RhoA (T19N), or expression of active Rac1 (Q61L), decreased basal and TSA-sensitive H3 and K9-H3 acetylations in suspended cells, but caused a slight increase in the TSA-insensitive histone acetylations in fibronectin-adherent cells. RhoA T19N expression did not alter the acetylations in adhered cells, unlike other cases of intracellular contractility down-regulation, presumably due to the complex nature of the RhoA downstream signaling and its complicate kinetic activity profile as cells adhere (31). The ML9-mediated changes in H3 and K9-H3 acetylations correlated with increased HDACs activity in suspended cells, and decreased activity in adherent cells by ML9 treatment. Further, enhancement of the contractility via MLCK overexpression or CaMKII inhibition by KN93 resulted in increased basal and TSA-sensitive histone H3 and K9-H3 acetylations in the suspended cells, although the fibronectin-adherent cells showed no significant changes in the minimal and TSA-insensitive acetylations.

It was shown that fibronectin-adherent SNU16mAd cells were not significantly sensitive to TSA, resulting in no significant changes in HDACs activity, histone acetylation on TSA treatment (Figures 2, 3, and 4), and regulation of intracellular contractility (e.g., ROCK1 expression, Figure 5). At this time, it is not clear how the fibronectin-adherent cells were insensitive to TSA treatment for the effects, whereas suspended cells were sensitive. It may not be ruled out that the reason may be related with the fact that the unique SNU16mAd cell line was derived from an anchorage-independent cell line, presumably which the anchorage-requirement for their growth and/or other cellular functions was somehow overcome during carcinogenetic processes. Therefore, the lack of change in TSA-mediated acetylation

in fibronectin-adherent cells might be because adhesion signaling was not sufficient for SNU16mAd cells to show the TSA response. Interestingly, TSA-sensitivity of the acetylation in suspended cells became less TSA-sensitive when certain treatments was applied to regulate cellular contractility. In case of treatments of ML9, Ac-H3 and Ac-K9-H3 became TSA-insensitive, whereas Y27632 or calmidazolium treatment or Rac1 Q61L transfection resulted in TSA-insensitive Ac-H3 but -sensitive Ac-K9-H3 in suspended cells, indicating their complicate roles in the regulation of cellular contractility.

We observed higher MLC phosphorylation in anchorage-independent cells or suspended gastric carcinoma cells. It is consistent with a previous report showing that Swiss 3T3 cells suspended for 18 h showed higher phosphorylations in MLC, indicating an excessively higher contractility, compared to adherent cells (32). Although RhoA pathway impaired in suspended fibroblast cells might not support MLC phosphorylation (ppThr¹⁸Ser¹⁹MLC), MLCK- or ROCK-mediated pSer¹⁹MLC or pThr¹⁸MLC and thereby intracellular contractility might still be maintained in suspended cells to retract cell surface for a round shape (33). TSA-treatment in suspended cells further appeared to increase intracellular contractility. The TSA-mediated increase in the contractility may somehow affect nuclear architecture and biochemistry, leading to decreased HDACs activity, an enhanced histone

acetylation, and expression of genes involved in maintenance of cellular functions. This is evidenced by increased epigenetic expression of signaling molecules including ROCK1 and concomitant MLC phosphorylation. In turn, the activities of contractility-related signaling molecules appeared to modulate cell adhesion ability. Activation of the contractility-related molecules decreased cell adhesion on fibronectin, whereas inhibition of them increased the adhesion. Meanwhile, it may be speculated that TSA treatment may regulate cell adhesion if ROCK1 is a key target. Therefore, the cell adhesion status-dependent and cellular contractility-mediated modulation of H3 and K9-H3 acetylations appears to regulate, through a feedback loop, the expression of genes implicated in cytoskeletal reorganization and thereby contractility as cells adhere.

All together, these data clearly indicate a close functional linkage of histone acetylation with cell adhesion-dependent signal transduction for intracellular contractility. Cells under contractile forces may induce alterations in the organization of signaling or structural modules in focal adhesions or hemidesmosomes, or function to disrupt linkages that destabilize these structures (5). Therefore, alterations in global intracellular contractility and signaling environments may eventually affect nuclear architecture and function through nuclear matrix and histone modification or reorganization (34).

REFERENCES

1. Brakebusch, C., and Fassler, R. (2003) *EMBO J.* **22**, 2324-2333
2. Carragher, N. O., Westhoff, M. A., Fincham, V. J., Schaller, M. D., and Frame, M. C. (2003) *Curr. Biol.* **13**, 1442-1450
3. Juliano, R. L., Reddig, P., Alahari, S., Edin, M., Howe, A., and Aplin, A. (2004) *Biochem. Soc. Trans.* **32**, 443-446
4. Lee, J. W., and Juliano, R. (2004) *Mol. Cells* **17**, 188-202
5. Balda, M. S., and Matter, K. (2003) *Trends Cell Biol.* **13**, 310-318
6. Muller, J. M., Metzger, E., Greschik, H., Bosserhoff, A. K., Mercep, L., Buettner, R., and Schule, R. (2002) *EMBO J.* **21**, 736-748
7. Fischle, W., Wang, Y., and Allis, C. D. (2003) *Curr. Opin. Cell Biol.* **15**, 172-183
8. Felsenfeld, G., and Groudine, M. (2003) *Nature* **421**, 448-453
9. Egger, G., Liang, G., Aparicio, A., and Jones, P. A. (2004) *Nature* **429**, 457-463
10. Ehrenhofer-Murray, A. E. (2004) *Eur. J. Biochem.* **271**, 2335-2349
11. Geiman, T. M., and Robertson, K. D. (2002) *J. Cell Biochem.* **87**, 117-125
12. Vermaak, D., Ahmad, K., and Henikoff, S. (2003) *Curr. Opin. Cell Biol.* **15**, 266-274

13. Iizuka, M., and Smith, M. M. (2003) *Curr. Opin. Genet. Dev.* **13**, 154-160
14. Kamm, K. E., and Stull, J. T. (2001) *J. Biol. Chem.* **276**, 4527-4530
15. Pfitzer, G. (2001) *J. Appl. Physiol.* **91**, 497-503
16. Schoenwaelder, S. M., and Burridge, K. (1999) *Curr Opin Cell Biol* **11**, 274-286.
17. Olson, M. F. (2004) *Trends Cell Biol.* **14**, 111-114
18. McKinsey, T. A., Zhang, C.-L., Lu, J., and Olson, E. N. (2000) *Nature* **408**, 106-111
19. Allard, S., Masson, J. Y., and Cote, J. (2004) *Biochim. Biophys. Acta* **1677**, 158-164
20. Lee, M. S., Ko, S. G., Kim, H. P., Kim, Y. B., Lee, S. Y., Kim, S. G., Jong, H. S., Kim, T. Y., Lee, J. W., and Bang, Y. J. (2004) *Int. J. Oncol.* **24**, 1229-1234
21. Lee, J. W., and Juliano, R. L. (2000) *Mol. Biol. Cell* **11**, 1973-1987.
22. Lee, J. W., and Juliano, R. L. (2002) *Biochim. Biophys. Acta* **1542**, 23-31.
23. Nielsen, A. L., Ortiz, J. A., You, J., Oulad-Abdelghani, M., Khechumian, R., Gansmuller, A., Chambon, P., and Losson, R. (1999) *EMBO J.* **18**, 6385-6395
24. Ye, S.-K., Agata, Y., Lee, H.-C., Kurooka, H., Kitamura, T., Shimizu, A., Honjo, T., and Ikuta, K. (2001) *Immunity* **15**, 813-823
25. Kim, H. P., Lee, M. S., Yu, J., Park, J. A., Jong, H. S., Kim, T. Y., Lee, J. W., and Bang, Y. J. (2004) *Biochem. J.* **379**, 141-150
26. Marks, P. A., Miller, T., and Richon, V. M. (2003) *Curr. Opin. Pharmacol.* **3**, 344-351
27. Marks, P., Rifkind, R. A., Richon, V. M., Breslow, R., Miller, T., and Kelly, W. K. (2001) *Nat. Rev. Cancer* **1**, 194-202
28. Galasinski, S. C., Resing, K. A., Goodrich, J. A., and Ahn, N. G. (2002) *J. Biol. Chem.* **277**, 19618-19626
29. van Leeuwen, F. N., Kain, H. E., Kammen, R. A., Michiels, F., Kranenburg, O. W., and Collard, J. G. (1997) *J. Cell Biol.* **139**, 797-807
30. van Leeuwen, F. N., van Delft, S., Kain, H. E., van der Kammen, R. A., and Collard, J. G. (1999) *Nat. Cell Biol.* **1**, 242-248
31. Arthur, W. T., and Burridge, K. (2001) *Mol. Biol. Cell* **12**, 2711-2720.
32. Ren, X. D., Kiosses, W. B., and Schwartz, M. A. (1999) *EMBO J.* **18**, 578-585
33. Ren, X.-D., Wang, R., Li, Q., Kahek, L. A. F., Kaibuchi, K., and Clark, R. A. F. (2004) *J. Cell Sci.* **117**, 3511-3518
34. Boudreau, N., Myers, C., and Bissell, M. J. (1995) *Trends Cell Biol.* **5**, 1-4

FOOTNOTES

We authors thank Dr. Sarah M. Short (Children's Hospital, Harvard Medical School, Boston, MA) and Dr. Eun-Kyung Suh (Harvard Medical School, Boston, MA) for helpful discussions and review of the manuscript. This study was supported by a grant of the 2003 National R&D Program for Cancer Control, Ministry of Health & Welfare, Republic of Korea. to JW Lee (0320040-2).

FIGURE LEGENDS

Figure 1. Cell adhesion status-dependent histone H3 and K9-H3 acetylations. SNU16mAd cells were either kept in suspension (Sus) or replated on fibronectin- (10 $\mu\text{g/ml}$, Fn) precoated culture dishes. After incubation for the indicated periods, nuclear extracts were prepared and used for immunoblots with antibodies against the indicated molecules (A & B) or HDAC activity assays (C), as explained in the Experimental Procedures. The mean \pm standard deviation (SD) values (A, n = 4) were shown under the Ac-H3 immunoblot and as following from left to right (1.0 \pm 0.04, 0.35 \pm 0.03, 0.82 \pm 0.06, 0.10 \pm 0.03, 1.0 \pm 0.06, and 0.02 \pm 0.01). (B) Data shown are representative of three independent experiments. (C) Data are shown as means \pm SD and are representative of three isolated experiments performed in triplicate. *p* values for * (≤ 0.05) and *p* values ≤ 0.05 were considered significant (A and C, respectively).

Figure 2. TSA-sensitive histone H3 and K9-H3 acetylations in suspended, but not in fibronectin-adherent, cells. (A) Basal and TSA-mediated histone H3 and K9-H3 acetylations dependent of cell adhesion status-. Cell manipulation and treatments of TSA at 100 nM were done as explained in the Experimental Procedures. The mean \pm SD values ($n = 5$) under the Ac-H3 immunoblot were as following from left to right (1.0 ± 0.02 , 1.73 ± 0.10 , 0.11 ± 0.04 , and 0.13 ± 0.03). (B) Nuclear extracts prepared were processed for the HDACs assay, as explained in the Experimental Procedures. Relative TSA efficiency $[(F_{TSA}-F_{vehicle})/F_{vehicle}]$ was calculated and plotted. F_{TSA} : Fluorescence at 460 nm for 100 nM TSA-treated condition, $F_{vehicle}$: Fluorescence at 460 nm for vehicle DMSO-treated condition. (C) Cells were untreated or pretreated with cytochalasin D (CytoD, 1.0 μ M) or okadaic acid (OK, 150 nM), 30 min prior to the replating and incubation at 37°C for 20 h. The mean \pm SD values ($n = 3$) were shown under the Ac-H3 immunoblot and as following from left to right (0.07 ± 0.02 , 0.04 ± 0.01 , 1.0 ± 0.05 , 0.12 ± 0.02 , 1.0 ± 0.07 , 0.0 ± 0.005 , and 0.98 ± 0.05). (A, B, and D) p values ≤ 0.05 were considered significant; p values for * were ≤ 0.05 , indicating their significance.

Figure 3. Intracellular contractility-related signaling activities via MLCK regulate HDACs activity and histone acetylation. SNU16mAd cells were pretreated with 25 μ M ML9 (A), 20 μ M KN93 (E), 20 μ M KN92 (F), or 30 μ M calmidazolium (G), 30 min before either being kept in suspension (Sus) or replated onto fibronectin (Fn) without or with TSA treatment. Data are representative of three different experiments. The mean \pm SD values (A, $n = 3$) under the Ac-H3 immunoblot were as following from left to right (1.0 ± 0.03 , 2.98 ± 0.21 , 0.11 ± 0.01 , 0.07 ± 0.02 , 0.32 ± 0.03 , 0.37 ± 0.02 , 0.35 ± 0.03 , and 0.32 ± 0.02). (B and C) Nuclear extracts prepared were processed for the HDACs assay, as explained in the Experimental Procedures. Data shown (mean \pm standard deviation) are representative from three independent experiments. p values ≤ 0.05 were considered significant. (D) Cells were transiently transfected with a control vector (Mock) or MLCK WT plasmids, 24 h before the cell replating. The mean \pm SD values (D, $n = 3$) under the Ac-H3 immunoblot were as following from left to right (1.0 ± 0.04 , 2.86 ± 0.13 , 0.01 ± 0.005 , 0.02 ± 0.01 , 0.51 ± 0.03 , 0.69 ± 0.02 , 0.24 ± 0.02 , and 0.29 ± 0.03). (A to G) p values ≤ 0.05 were considered significant; p values for * were ≤ 0.05 , and p values for # were ≥ 0.05 , indicating their significance and non-significance, respectively. The mean \pm SD values (E, $n = 3$) under the Ac-H3 immunoblot were as following from left to right (1.0 ± 0.03 , 3.61 ± 0.23 , 0.01 ± 0.002 , 0.01 ± 0.004 , 1.53 ± 0.03 , 6.89 ± 0.29 , 0.01 ± 0.002 , and 0.01 ± 0.003). The mean \pm SD values (F, $n = 3$) under the Ac-H3 immunoblot were as following from left to right (1.0 ± 0.04 , 3.56 ± 0.14 , 0.05 ± 0.02 , 0.01 ± 0.007 , 1.11 ± 0.07 , 3.79 ± 0.22 , 0.04 ± 0.02 , and 0.01 ± 0.007). (G) p value of & was non-significantly ≥ 0.05 for Ac-H3 but significantly ≤ 0.05 for Ac-K9-H3. The mean \pm SD values (G, $n = 3$) under the Ac-H3 immunoblot were as following from left to right (1.0 ± 0.02 , 2.86 ± 0.21 , 0.01 ± 0.003 , 0.02 ± 0.008 , 0.51 ± 0.08 , 0.69 ± 0.09 , 0.24 ± 0.02 , and 0.29 ± 0.05).

Figure 4. Intracellular contractility-related signaling activities involving RhoA pathways regulate HDACs activity and histone acetylation. SNU16mAd cells were transiently transfected with a control vector (Mock) or RhoA T19N (A), with control siRNA or ROCK1 siRNA (C), or with control vector (Mock) or Rac1 Q61L (D) plasmids, 24 h before either being kept in suspension (Sus) or replated onto fibronectin (Fn) without or with TSA treatment. The mean \pm SD values (A, $n = 3$) for the Ac-H3 immunoblot were as following from left to right (1.0 ± 0.03 , 5.73 ± 0.34 , 0.03 ± 0.01 , 0.01 ± 0.009 , 0.33 ± 0.04 , 2.09 ± 0.19 , 0.01 ± 0.002 , and 0.01 ± 0.004). (B) Cells were pretreated with 15 μ M Y27632, 30 min before either being kept in suspension (Sus) or replated onto fibronectin (Fn) without or with TSA treatment. The mean \pm SD values (B, $n = 3$) for the Ac-H3 immunoblot were as following from left to right (1.0 ± 0.05 , 2.16 ± 0.12 , 0.06 ± 0.01 , 0.08 ± 0.02 , 0.23 ± 0.04 , 0.30 ± 0.05 , 0.28 ± 0.02 , and 0.25 ± 0.04). The mean \pm SD values (C, $n = 3$) under the Ac-H3 immunoblot were as following from left to right (1.0 ± 0.02 , 2.73 ± 0.20 , 0.03 ± 0.01 , 0.01 ± 0.005 , 0.12 ± 0.03 , 0.46 ± 0.05 , 0.34 ± 0.02 , and 0.38 ± 0.05). The mean \pm SD values (D, $n = 3$) for the Ac-H3 immunoblot were as following from left to right (1.0 ± 0.02 , 2.62 ± 0.31 , 0.02 ± 0.01 , 0.01 ± 0.007 , 0.15 ± 0.03 , 0.18 ± 0.05 , 0.21 ± 0.03 , and 0.19 ± 0.02). (A to D) p values ≤ 0.05 were considered significant; p values for * were ≤ 0.05 , indicating their

significance. (B and D) p value of $\&$ was non-significantly ≥ 0.05 for Ac-H3 but significantly ≤ 0.05 for Ac-K9-H3.

Figure 5. Correlation of the histone acetylation and cell adhesion status-dependent expression of ROCK1. Cells were replated on fibronectin without or with TSA treatment as explained above. Data shown are representative from at least three independent experiments. (A) Chromatin immunoprecipitation of acetylated H3 or Lys9-acetylated H3 resulted in more co-precipitation of ROCK1 promoter regions in suspended cells in a TSA-sensitive manner, but not in Fn-adherent cells. (B) RT-PCR to detect ROCK1 showed more mRNA of ROCK1 in suspended cells dependent of HDACs activity, but not in Fn-adherent cells. GAPDH mRNA levels was also analyzed for a control. (C and D) ROCK1 protein expression and MLC phosphorylation was favored in suspended cells over Fn-adherent cells. Immunoblots for the indicated molecules were performed as described in the Experimental Procedures. p values ≤ 0.05 were considered significant; p values for * were ≤ 0.05 , but p values for # were ≥ 0.05 , indicating their significance and non-significance, respectively (C). The mean \pm SD values (C, $n = 3$) under the ROCK1 Western blot were as following from left to right (1.0 ± 0.03 , 2.04 ± 0.11 , 0.28 ± 0.08 , and 0.19 ± 0.03).

Figure 6. Intracellular contractility-related signaling activities inversely regulate cell adhesion. (A) Differential expression of ROCK1 protein between anchorage-independent (SNU16) and adherently-growing cells (SNU16mAd). Cell lysates were prepared from normal cultures and used in the immunoblots for the indicated molecules. Data are representative from three isolated experiments. (B) Regulation of intracellular contractility-related signaling activities modulates cell adhesion. Cells were pretreated without or with the indicated inhibitors or activators 30 min before being replated on fibronectin. Fifteen hours later, floating cells were washed out and adherent cells were fixed and stained with crystal violet. The degrees of stains were eventually read at 564 nm by a microplate reader for the relative cell adhesion, as explained previously (25). Data shown are representative from three independent experiments. p values for * were ≤ 0.05 and considered significant, compared to cell adhesion level of the control.

Figure 7. Working model for intracellular contractility to regulate HDACs activity and histone acetylation in suspended gastric carcinoma cells. Thick line connections indicate pathways to increase intracellular contractility and thereby presumably to down-regulate HDACs activity and to increase histone acetylation. Thin line connections are oppositely working. Pharmacological inhibitors used in the study were shown within rectangles.

Figure 1. Yong-Bae Kim et al., 2004

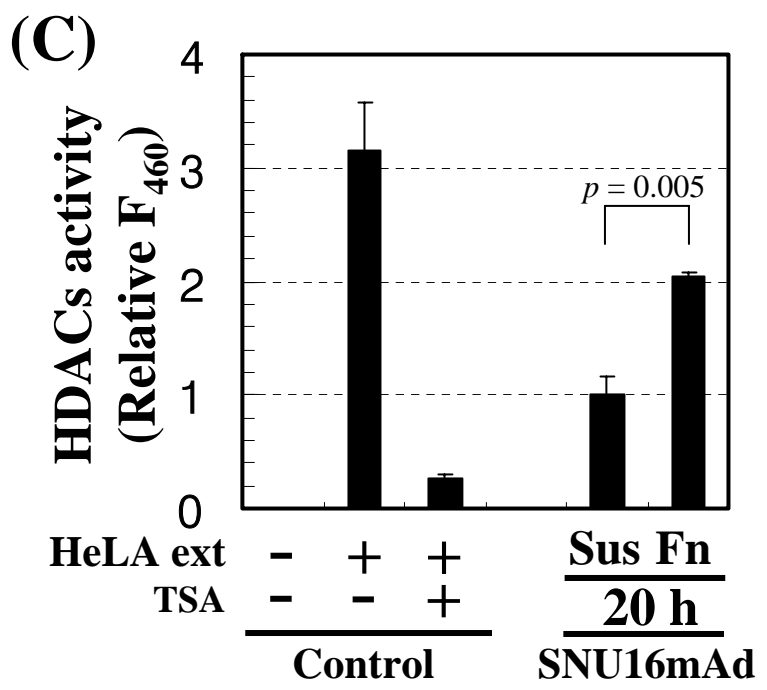
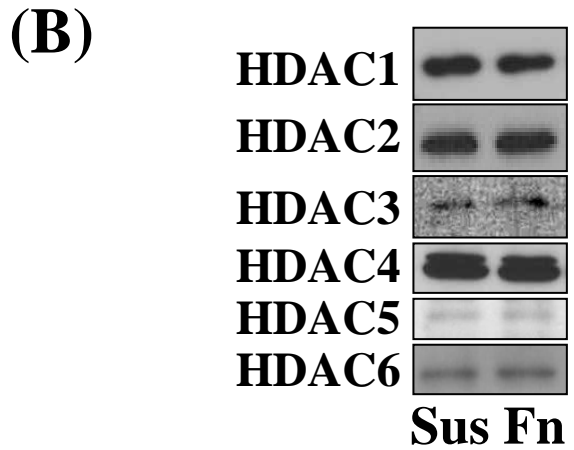
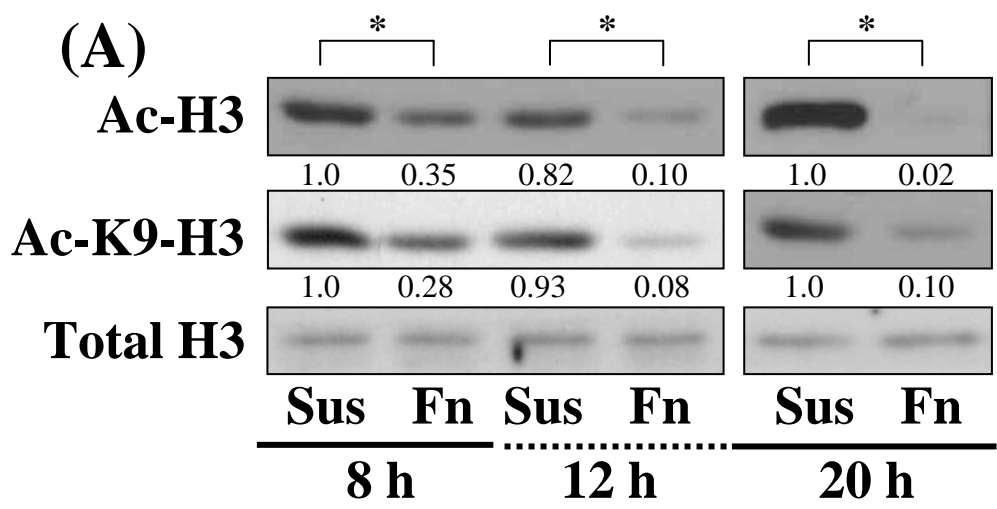
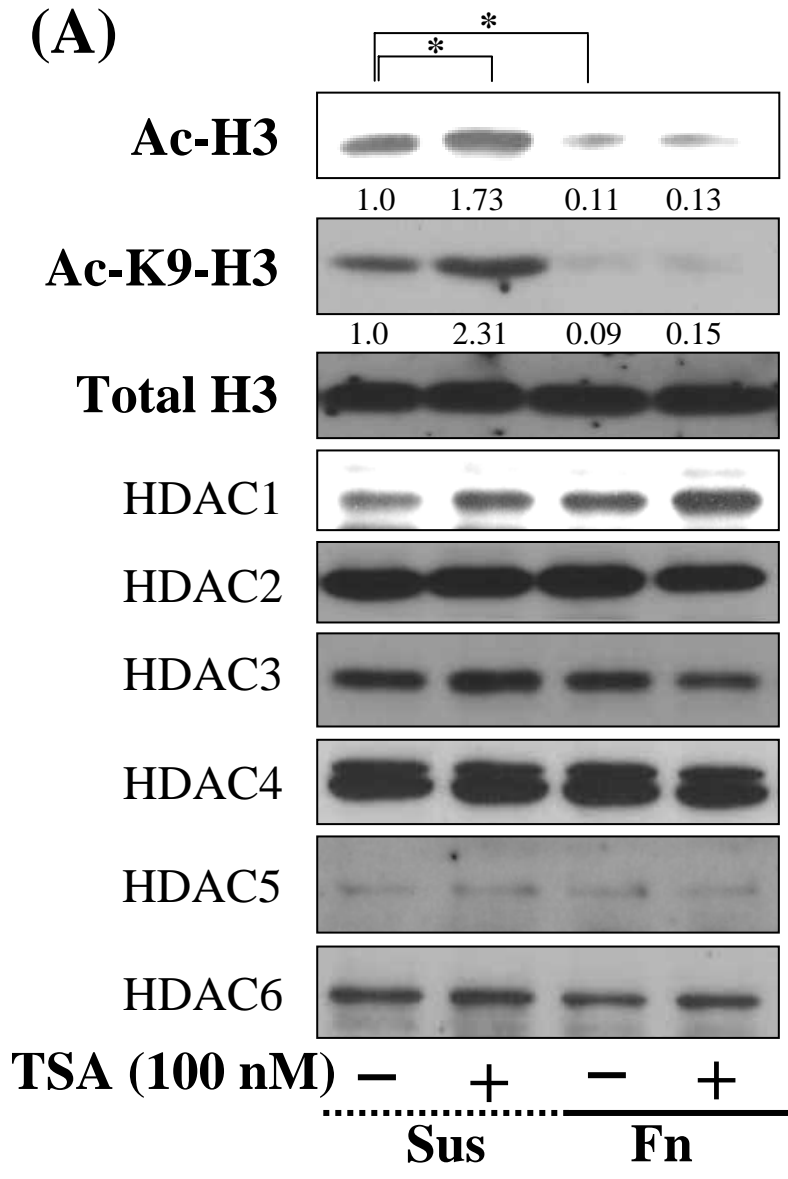
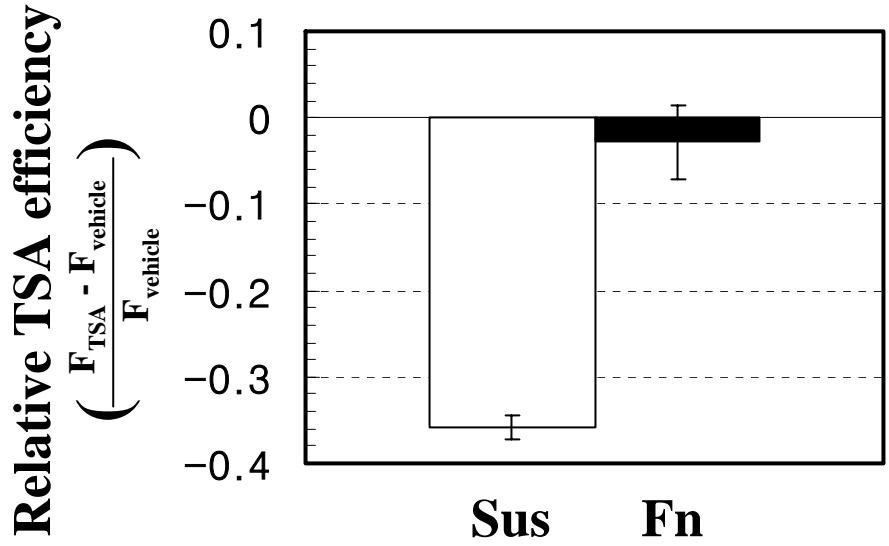


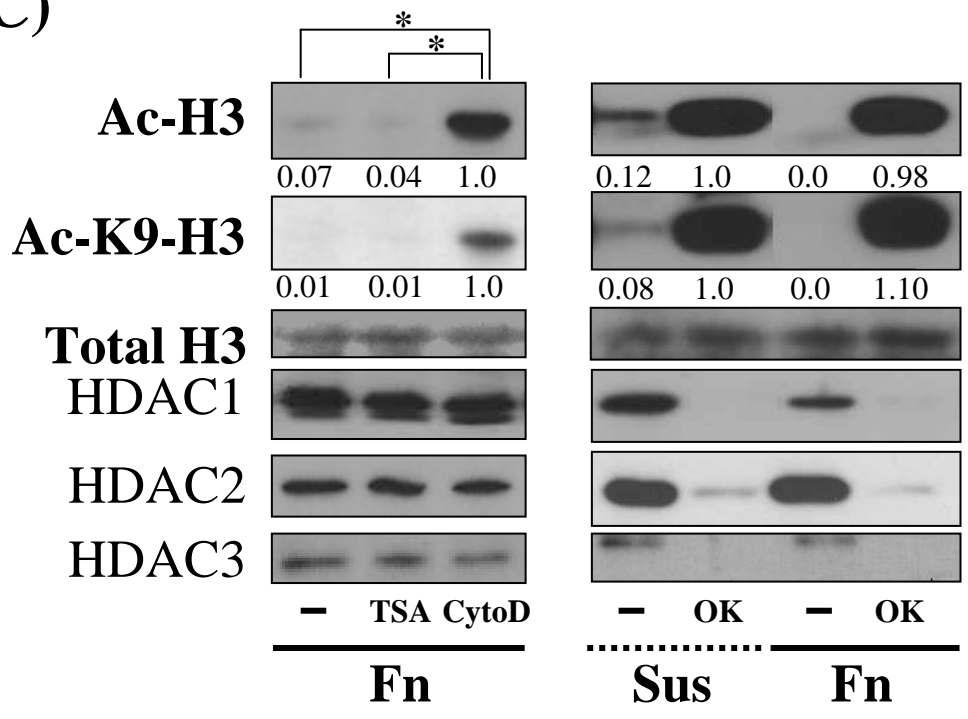
Figure 2. Yong-Bae Kim et al., 2004

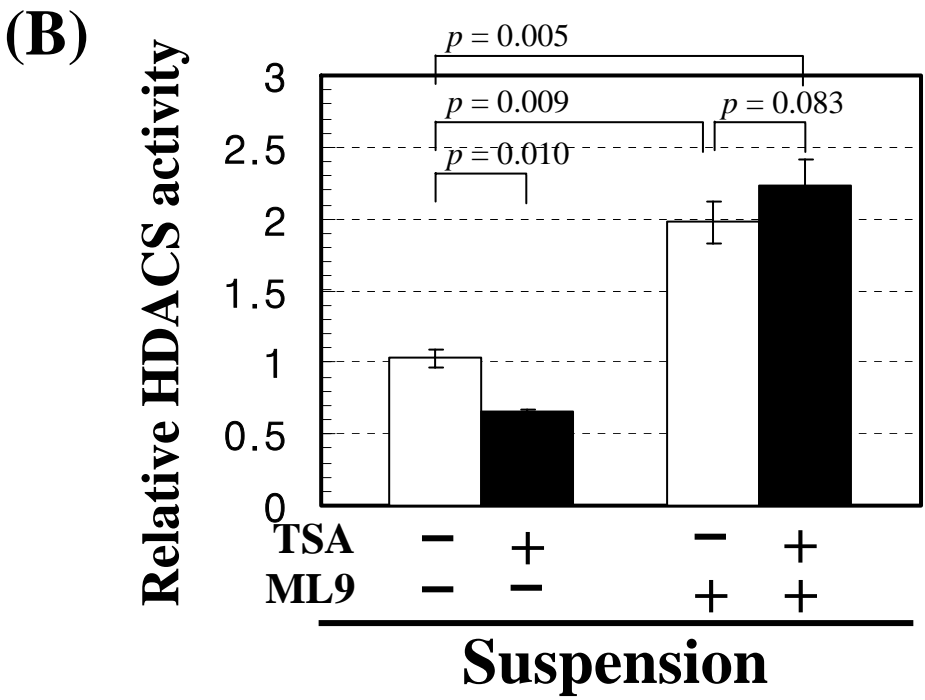
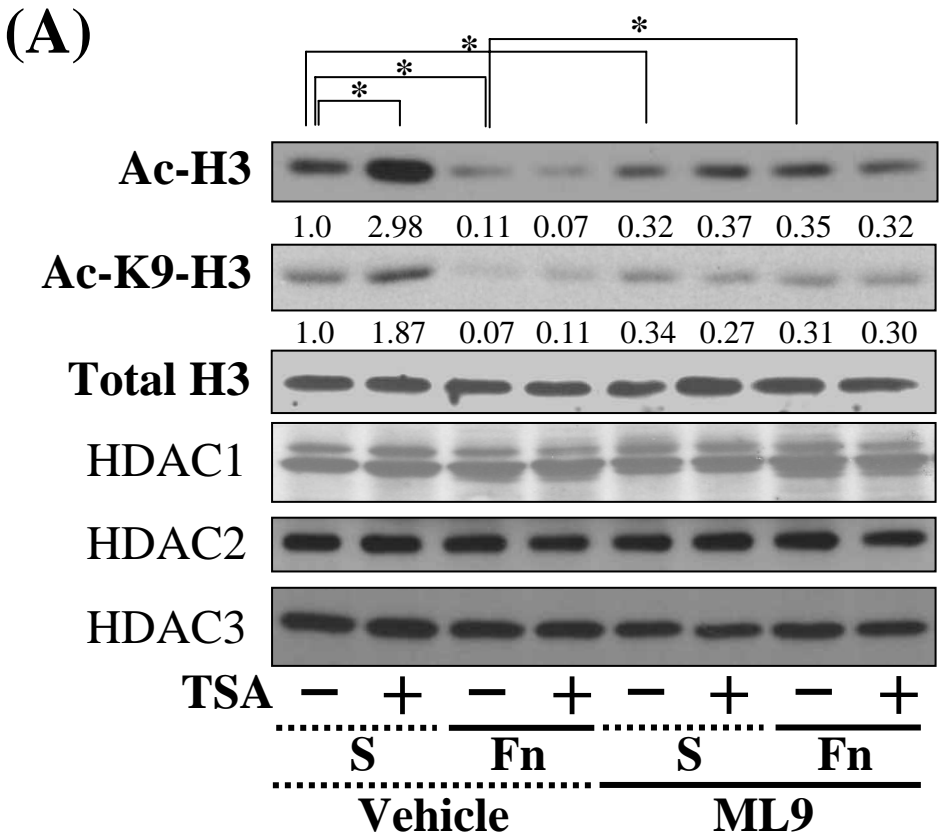


(B)

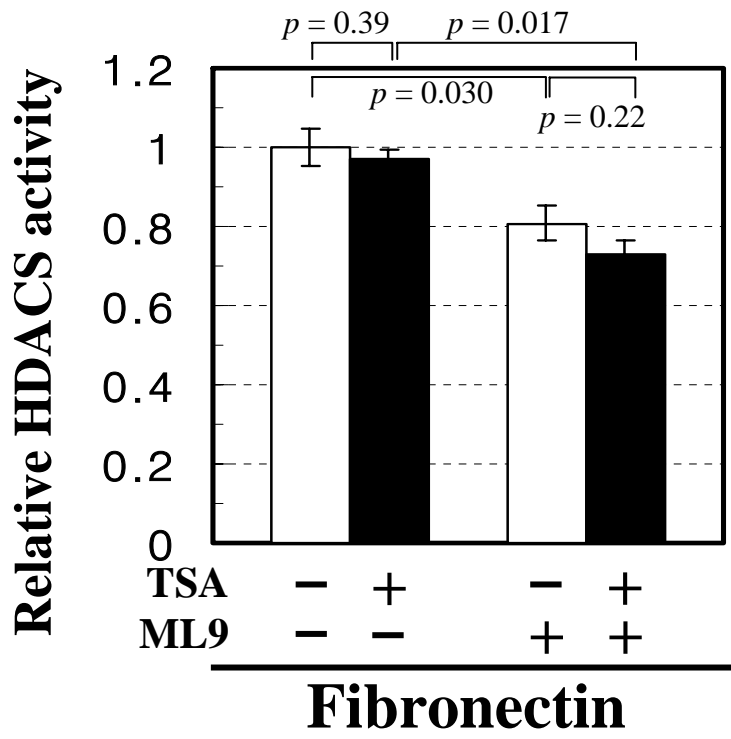


(C)

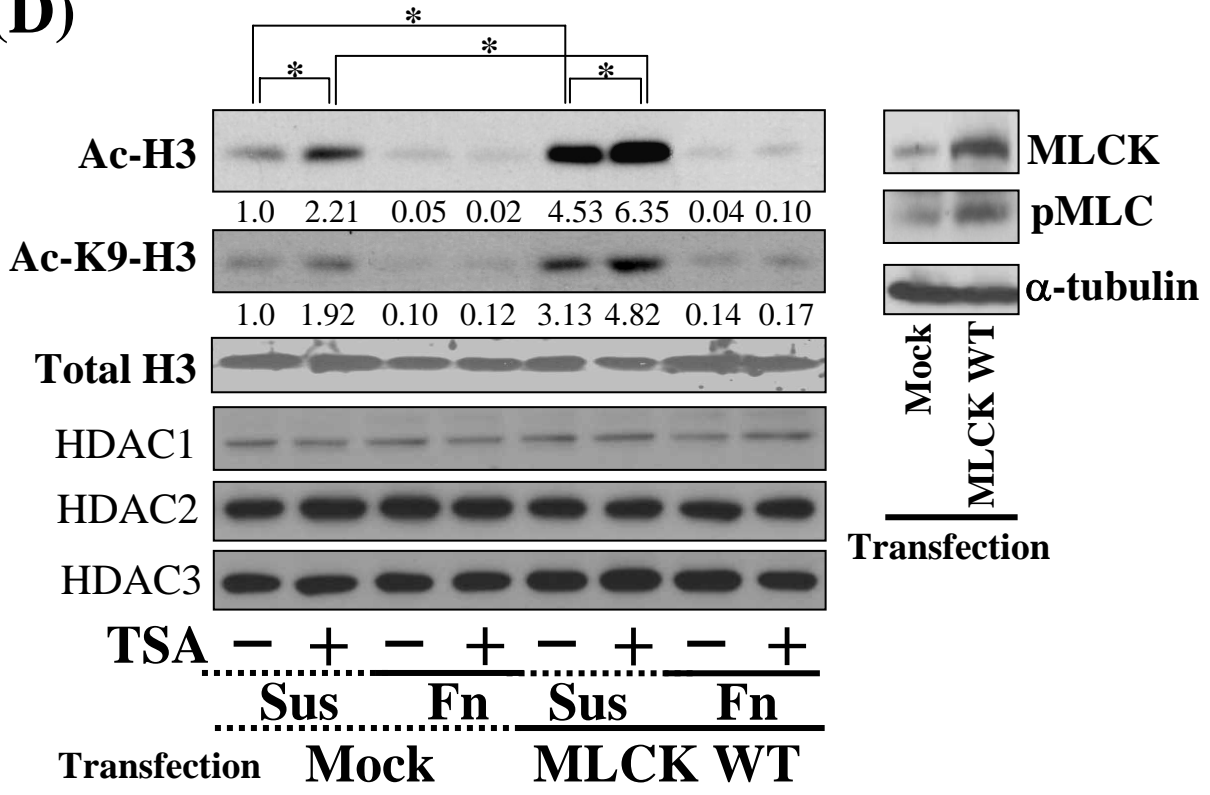


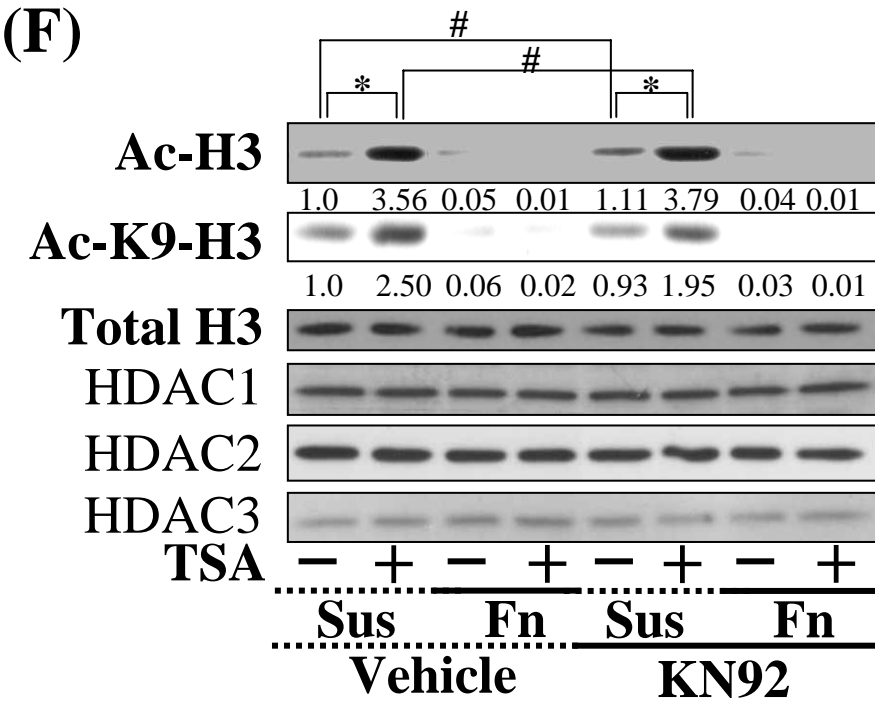
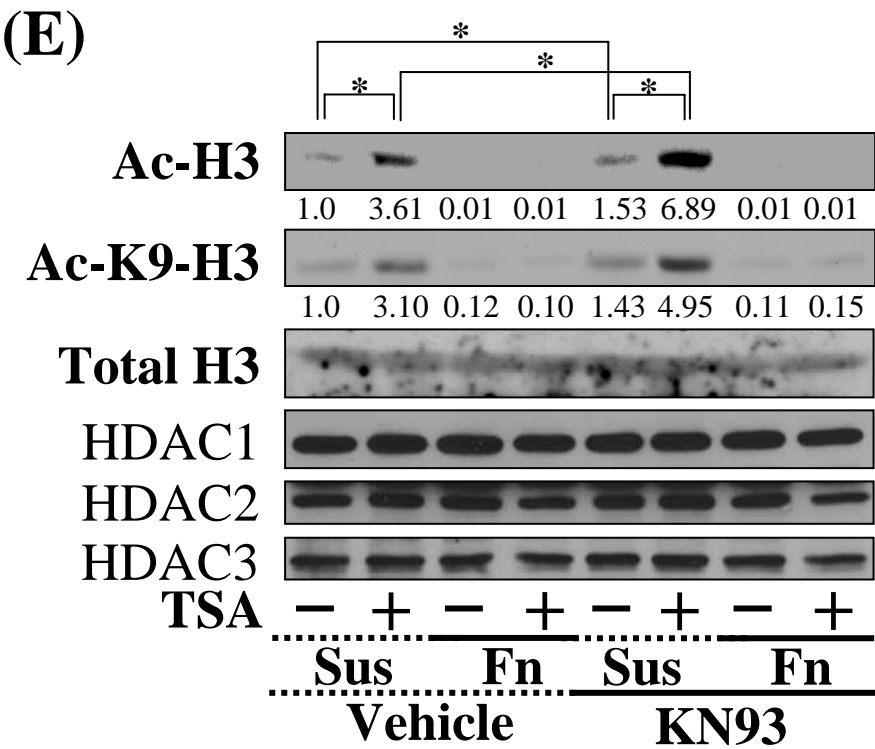


(C)

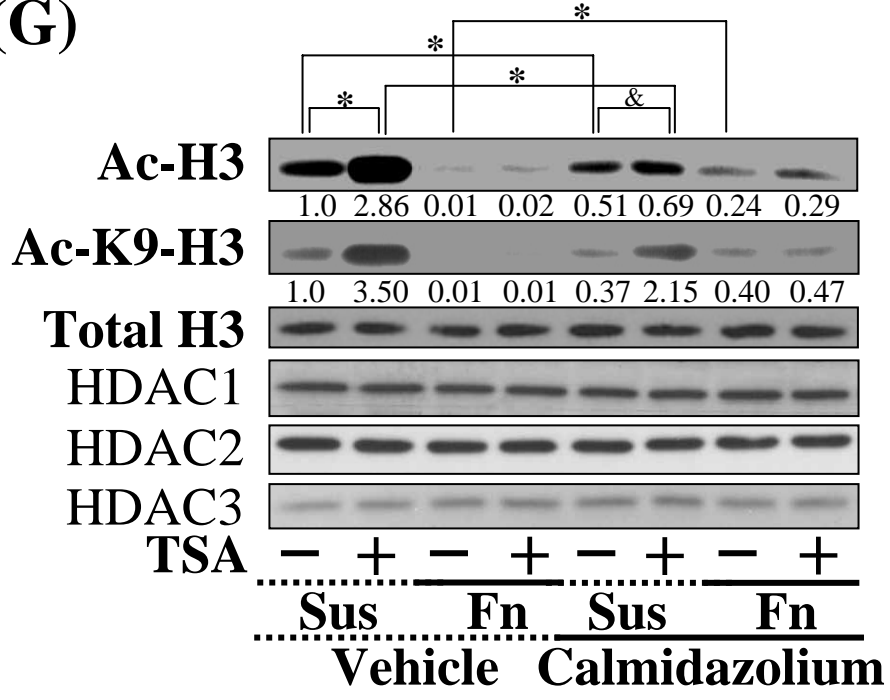


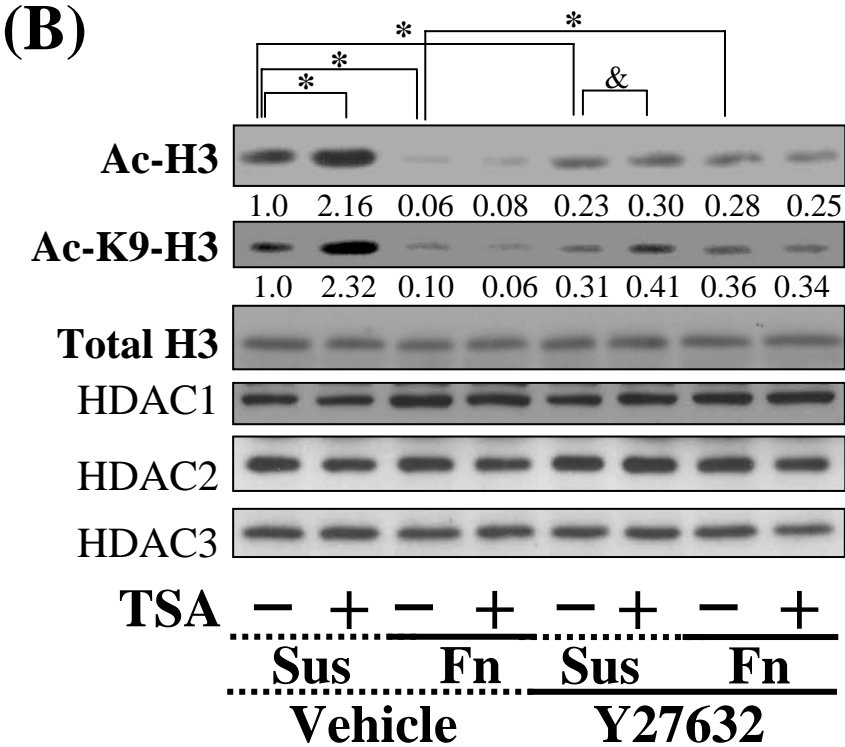
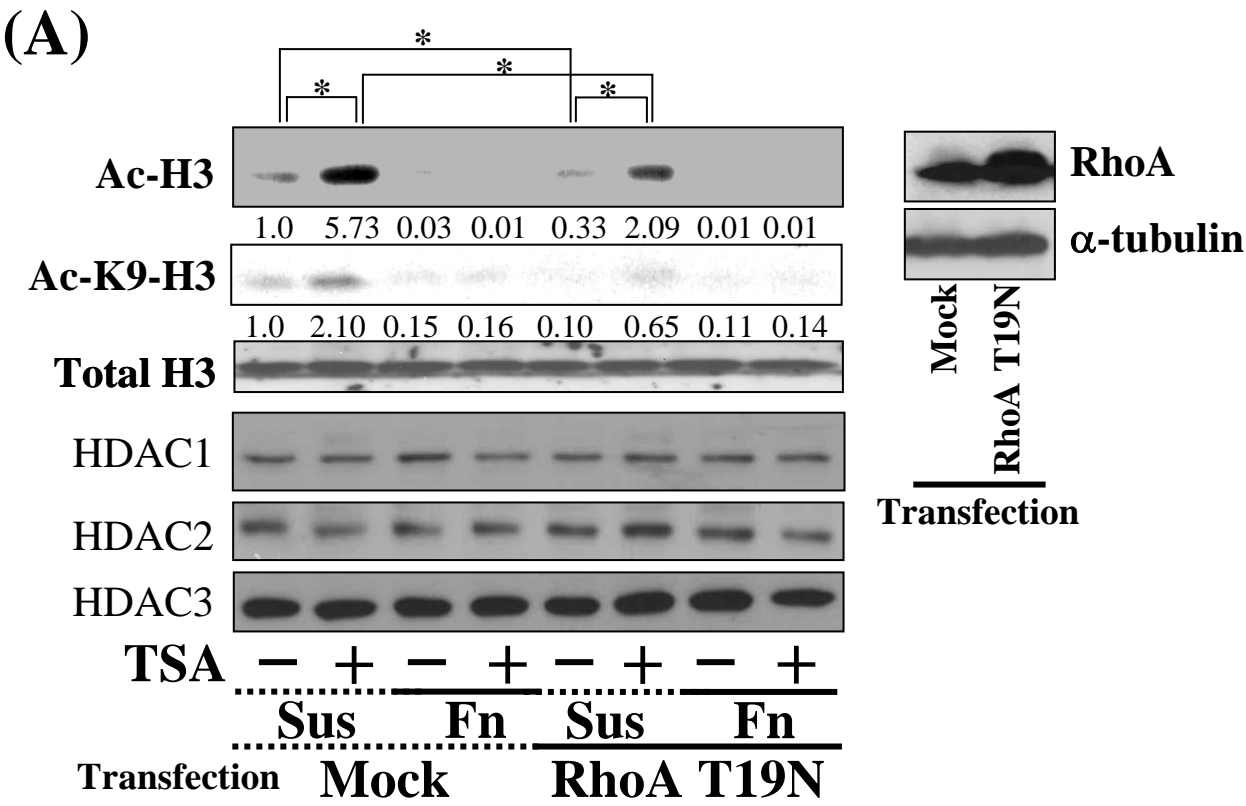
(D)



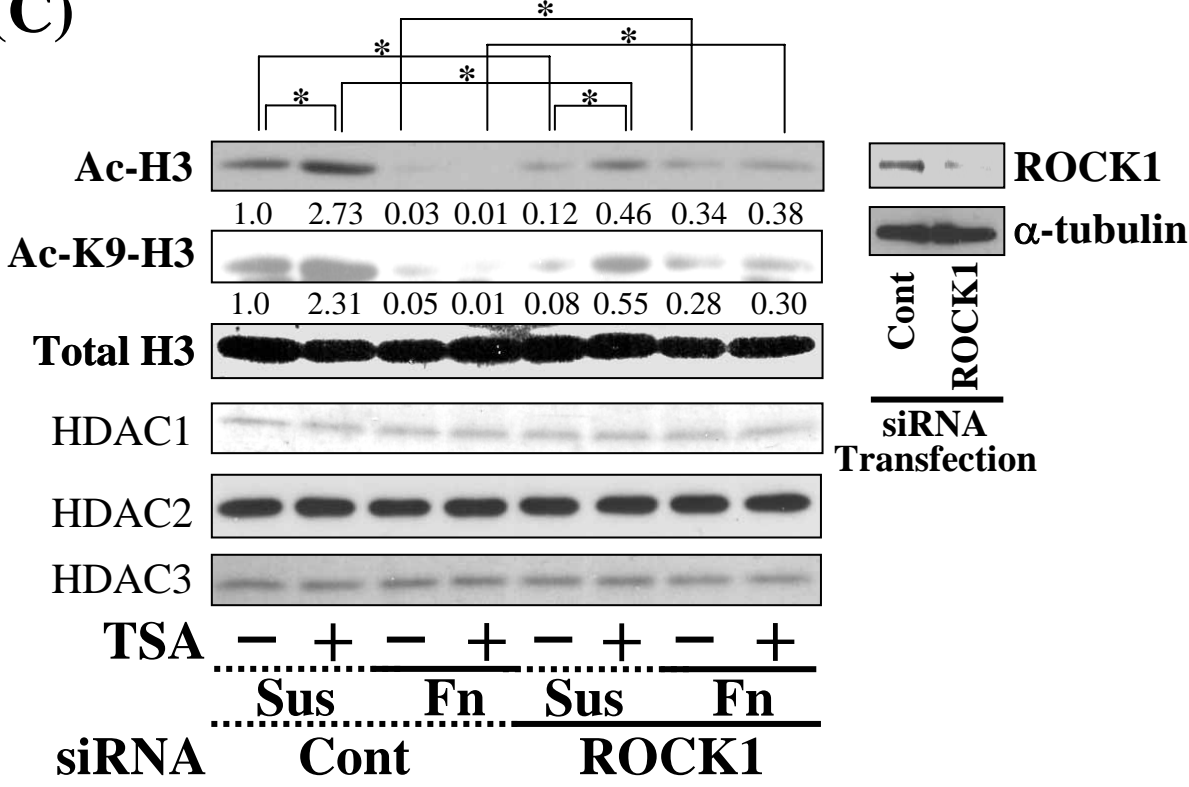


(G)





(C)



(D)

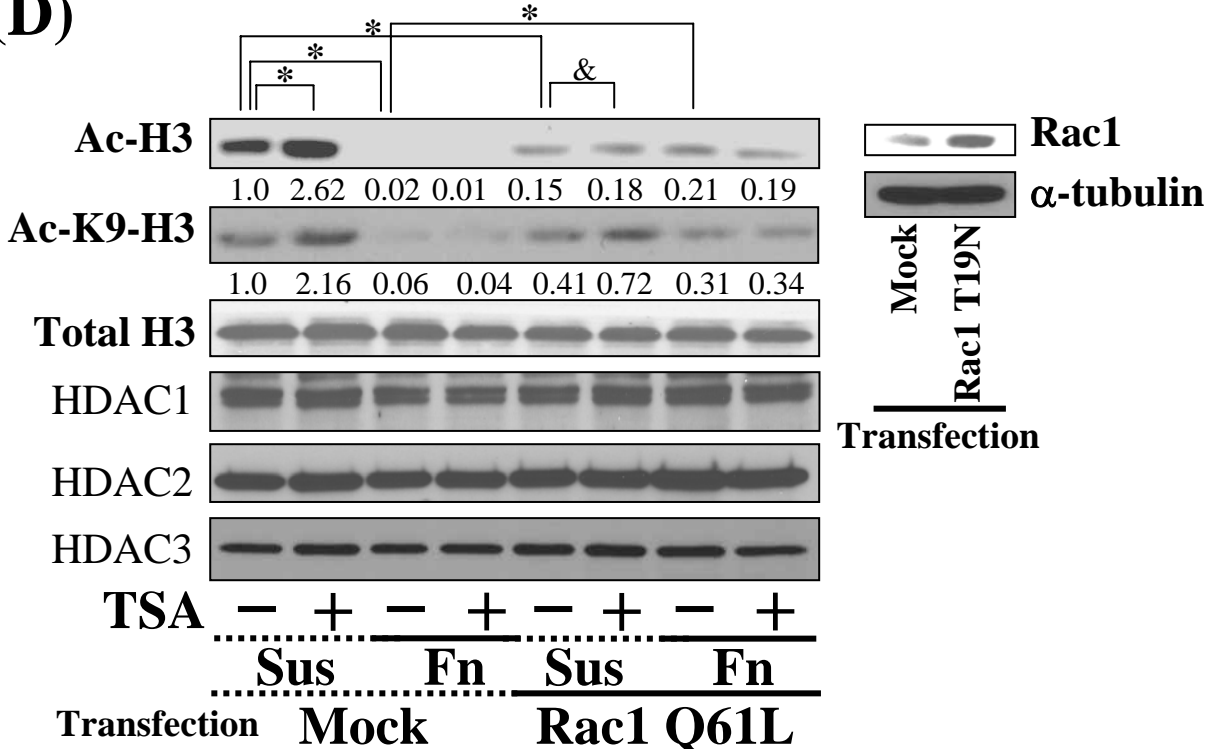
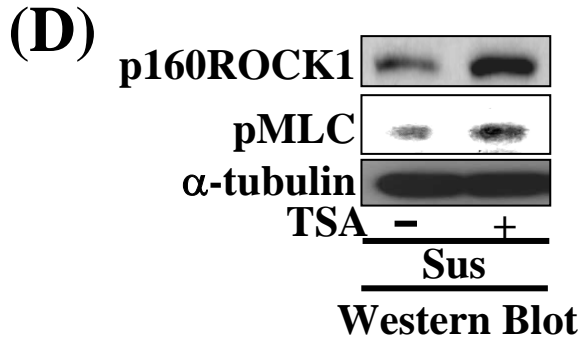
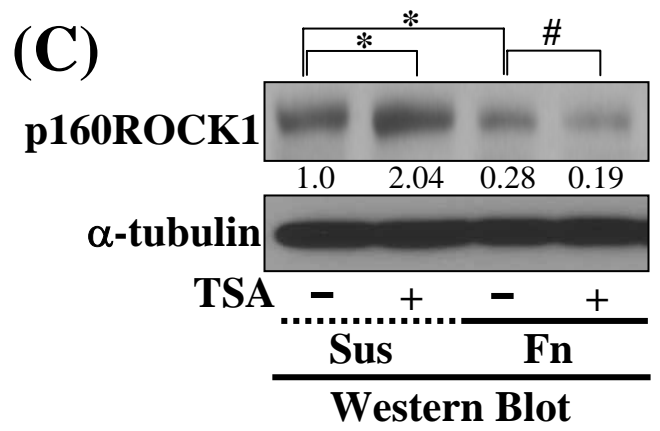
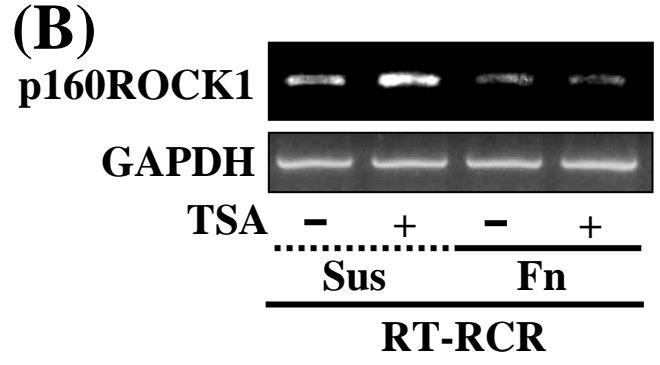
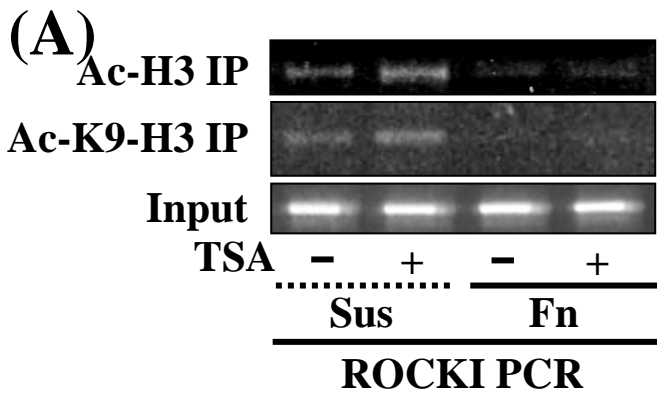


Figure 5. Yong-Bae Kim et al., 2004



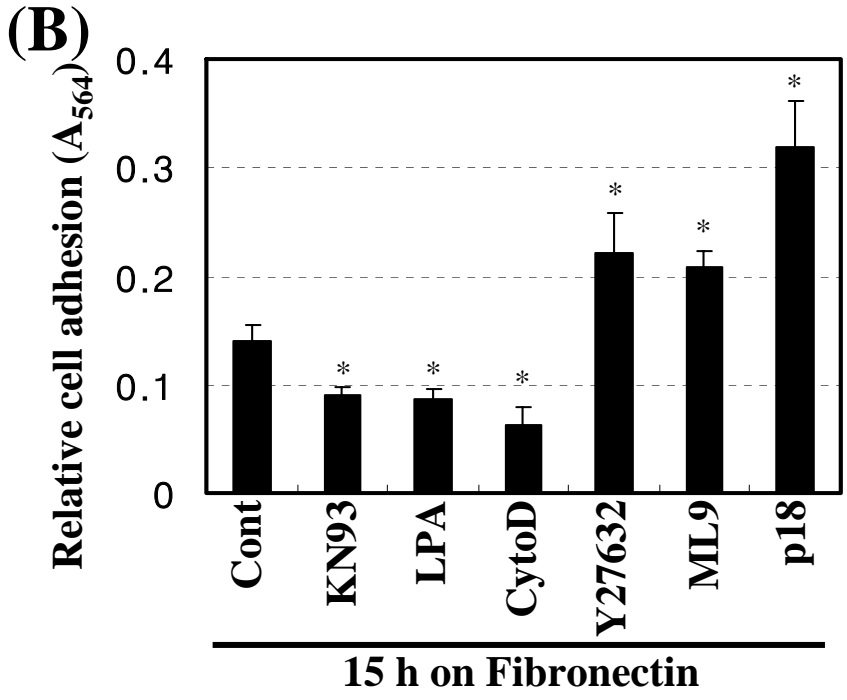
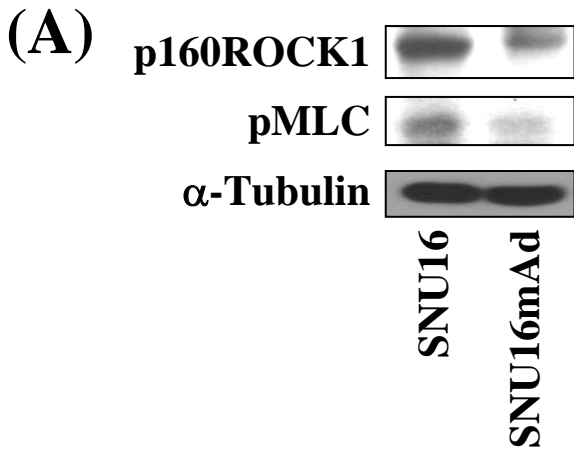


Figure 7. Yong-Bae Kim et al., 2004

